Composites Science and Technology 154 (2018) 110–116

Contents lists available at ScienceDirect

Composites Science and Technology

journal homepage: http://www.elsevier.com/locate/compscitech

The mechanics of reinforcement of polymers by graphene nanoplatelets

Robert J. Young*, Mufeng Liu, Ian A. Kinloch, Suhao Li, Xin Zhao, Cristina Vallés, Dimitrios G. Papageorgiou

National Graphene Institute and School of Materials, University of Manchester, Manchester M13 9PL, UK

ARTICLE INFO

Article history:
Received 2 October 2017
Received in revised form
8 November 2017
Accepted 9 November 2017
Available online 11 November 2017

Keywords:
Graphene
Nanocomposites
Elastic properties
Modelling
Raman spectroscopy

ABSTRACT

A detailed study has been undertaken of the mechanisms of stress transfer in polymeric matrices with different values of Young's modulus, E_m, reinforced by graphene nanoplatelets (GNPs). For each material, the Young's modulus of the graphene filler, E_f, has been determined using the rule of mixtures and it is found to scale with the value of E_m. Additionally stress-induced Raman bands shifts for the different polymer matrices show different levels of stress transfer from the polymer matrix to the GNPs, which again scale with E_m. A theory has been developed to predict the stiffness of the bulk nanocomposites from the mechanics of stress transfer from the matrix to the GNP reinforcement based upon the shear-lag deformation of individual graphene nanoplatelets. Overall it is found that it is only possible to realise the theoretical Young's modulus of graphene of 1.05 TPa for discontinuous nanoplatelets as E_m approaches 1 TPa; the effective modulus of the reinforcement will always be less for lower values of E_m. For flexible polymeric matrices the level of reinforcement is independent of the graphene Young's modulus and, in general, the best reinforcement will be obtained in nanocomposites with strong graphene-polymer interfaces and aligned nanoplatelets with high aspect ratios.

1. Introduction

Graphene has been found to have high levels of stiffness and strength [1] and so is an obvious candidate for the reinforcement of polymers [2–5]. Although there has been a rapid growth of interest in graphene-based polymer nanocomposites for structural applications [6], the mechanics of reinforcement in such materials is still not yet fully understood [7]. The mechanisms and mechanics of the reinforcement of polymers by 1D materials such as fibres has been studied widely [8] but as yet there is still no consensus about similar processes that may occur in nanocomposites reinforced by 2D materials such as a graphene.

There are generally two approaches that are used in considering the mechanical properties of polymer-based nanocomposites. Some people assume their mechanics to be similar to those of composites with macroscopic reinforcements, such as carbon and glass fibres [6,9,10]. Other researchers have taken an opposing viewpoint and have suggested polymer nanocomposites are actually quasi-homogeneous molecular blends that need to be regarded as molecular composites or self-reinforced composites [11,12]. In this case they have suggested that the classical micromechanical models developed for normal composites cannot be applied and that the properties are controlled by interactions on the molecular scale between the nanoparticles and the polymer matrix [12]. This approach has received considerable support particularly from groups working upon nanotube-based composites and there are clearly issues such as crystal nucleation and molecular confinement that cannot be explained through classical micromechanics [12]. In addition it has been pointed out that it is not yet clear as to why the promise of the 1 TPa Young's modulus of graphene is never realised during the reinforcement of nanocomposites [12].

In this present investigation, a detailed analysis has been undertaken of the mechanics and mechanisms of stress transfer in a range of polymeric matrices with very different levels of Young's modulus, E_m, reinforced by graphene nanoplatelets (GNPs). This use of matrix materials with a wide range of stiffnesses has allowed completely new insights into the mechanical properties of these technologically-important materials to be obtained. We produce overwhelming evidence to show that the elastic deformation of

* Corresponding author.
E-mail address: robert.young@manchester.ac.uk (R.J. Young).

https://doi.org/10.1016/j.compscitech.2017.11.007

graphene-reinforced polymers can be modelled using classical composite micromechanics [6,8,9], particularly at low levels of graphene loading. We will show to what extent this model can be employed and when other approaches may have to be used.

2. Experimental

2.1. Materials

The melt-processible thermoplastic elastomer (TPE) employed was Alcryn 2265 which is based on a partially cross-linked, chlorinated olefin interpolymer alloy. The polypropylene (PP) homopolymer employed was produced by Lyondellbasell under the commercial name, Moplen HP501L. Exfoliated graphite nanoplatelets (M25), produced by via the sulphuric intercalation of graphite, were obtained from XG Sciences (East Lansing, MI, USA). The M25 nanoplatelets are reported by XG Sciences to have an average thickness of 6–8 nm (~20 graphene layers) and they were found to have an average diameter of 7.7 μm (see Supplementary Information—Fig. S3). Since the M-grade materials have more than 10 graphene layers they should be termed "graphite nanoplatelets". They are, however, called "graphene nanoplatelets" by XG Sciences and since this terminology has been used widely in the literature, it will also be adopted in this present study.

2.2. Processing

The polymers were processed both neat and with different loadings of GNPs by a melt-mixing process performed using a twin-screw extruder (Thermo Scientific HAAKE MiniLab micro compounder) operated at 165 °C and 50 rpm for the TPE and at 190 °C and 100 rpm for the PP. The mixing of the GNPs into the polymers took place for 5 min for the TPE and 12 min for the PP. The pelletized products were further processed into dumbbell-shaped specimens by injection moulding (HAAKE MiniJet Piston Injection Moulding System) with $T_{cylinder} = 185$ °C, $T_{mould} = 30$ °C for the TPE and $T_{cylinder} = 200$ °C, $T_{mould} = 70$ °C for the PP.

2.3. Mechanical testing

Stress–strain curves were obtained using dogbone shaped specimens of both materials in an Instron 4301 machine, under a tensile rate of 50 mm min^{-1} with a load cell of 5 kN (ASTM D638).

2.4. Raman spectroscopy and deformation

For the TPE, samples were prepared as compression moulded sheets (185 °C). They were then stamped into small dumbbell-shape specimens with a gauge length of 10 mm marked by a pen on the specimens. They were then fixed in a mini tensile rig and the strain (extension between the two marks) was measured by a digital caliper. In the case of the PP, parallel sided bars were cut from middle of the dogbone tensile specimens and deformed in a four-point bending rig with the strain measured using a resistance strain gauge attached to the surface of the specimen. Raman spectra were obtained during deformation using a Renishaw inVia Raman microscope with a 633 nm laser.

3. Results and discussion

3.1. Young's modulus of the nanocomposites

One of the simplest relationships that has been developed to describe the reinforcement achieved from a high-modulus particulate filler in a low-modulus matrix, under uniform strain, is the so-called "rule of mixtures" (RoM), in which the Young's modulus of a composite E_c is given by Ref. [8].

$$E_c = E_f V_f + E_m\left(1 - V_f\right) \quad (1)$$

where E_f is the Young's modulus of the particulate filler, V_f is its volume fraction and E_m is the Young's modulus of the matrix. The Young's modulus of the filler E_f can be determined from a plot of E_c versus V_f. and examples of this are shown in Fig. 1 for graphene nanoplatelets (GNPs) in a thermoplastic elastomer (Alcryn − TPE) and polypropylene (PP). The stress-strain curves of the materials with different loadings of GNPs are shown in Fig. 1(a) and (b). The dependences of E_c upon V_f for the GNPs in the TPE and PP are shown in Fig. 1(c) and (d). It can be seen that for both systems there is an approximately linear increase in composite modulus with volume fraction up to a V_f of around 10%. The value of E_f for the GNPs in the polymers can be determined from the initial slope of these plots using Equation (1) and E_f ~ 400 MPa is determined for the TPE and ~15 GPa for the PP matrix. The first thing to point out is that the values of E_f determined for the two nanocomposite systems are well below the value of ~1 TPa reported [1] for the Young's modulus of graphene. It is more significant, however, that the value of E_f for the GNPs in the TPE is two orders of magnitude lower than that for the same nano-reinforcement in the PP which has a Young's modulus E_m two orders of magnitude higher than that of the TPE.

In this study we have determined E_f for a series of nanocomposites based upon a range of different polymers, including natural rubber [13], epoxy resins and another TPE (Pebax), all with very different values of E_m and reinforced with identical GNPs. The results are summarised in Table 1 where a very significant observation can be made. It can be seen that the values of E_f are highest for the materials with the highest matrix moduli, E_m. In fact there appears to be strong correlation between E_f and E_m − an order of magnitude decrease in E_m leads to an order of magnitude decrease in E_f. This observation is vital for our understanding of the mechanisms of deformation in these nanocomposites. We also recently pointed out that from the analysis of several hundred papers in the literature [14], that there is a general correlation between E_f and E_m for graphene-reinforced polymer nanocomposites. A log-log plot of literature values of E_f versus E_m for GNPs in a wide variety of different polymers is shown in Fig. S1 of the Supplementary Information. Although there is some scatter in the literature data, due presumably to different types of GNPs being used in the various studies, different processing conditions and variability in experimental procedures, it can nevertheless be seen that the data all fall on a straight line. In addition, the plot has a slope of the order of unity, showing that in general $E_f \propto E_m$.

3.2. Theoretical analysis

We have developed a comprehensive theory for the mechanisms of reinforcement of polymers by nanoplatelets that enables us to predict the effect of how reinforcement is controlled by factors such as matrix modulus, particle geometry and the strength of the filler-matrix interface. The basis of the theory is shown in Fig. 2. The individual nanoplatelets are assumed to be oriented randomly in the polymer matrix without interacting with each other as shown in the CT scan [13] in Fig. 2(a). In the case of nanocomposites containing particles such as graphene nanoplatelets, Equation (1) can be modified by replacing E_f with $E_{eff}\eta_o\eta_l$ to take into account the orientation of the reinforcing particles and their finite length to give

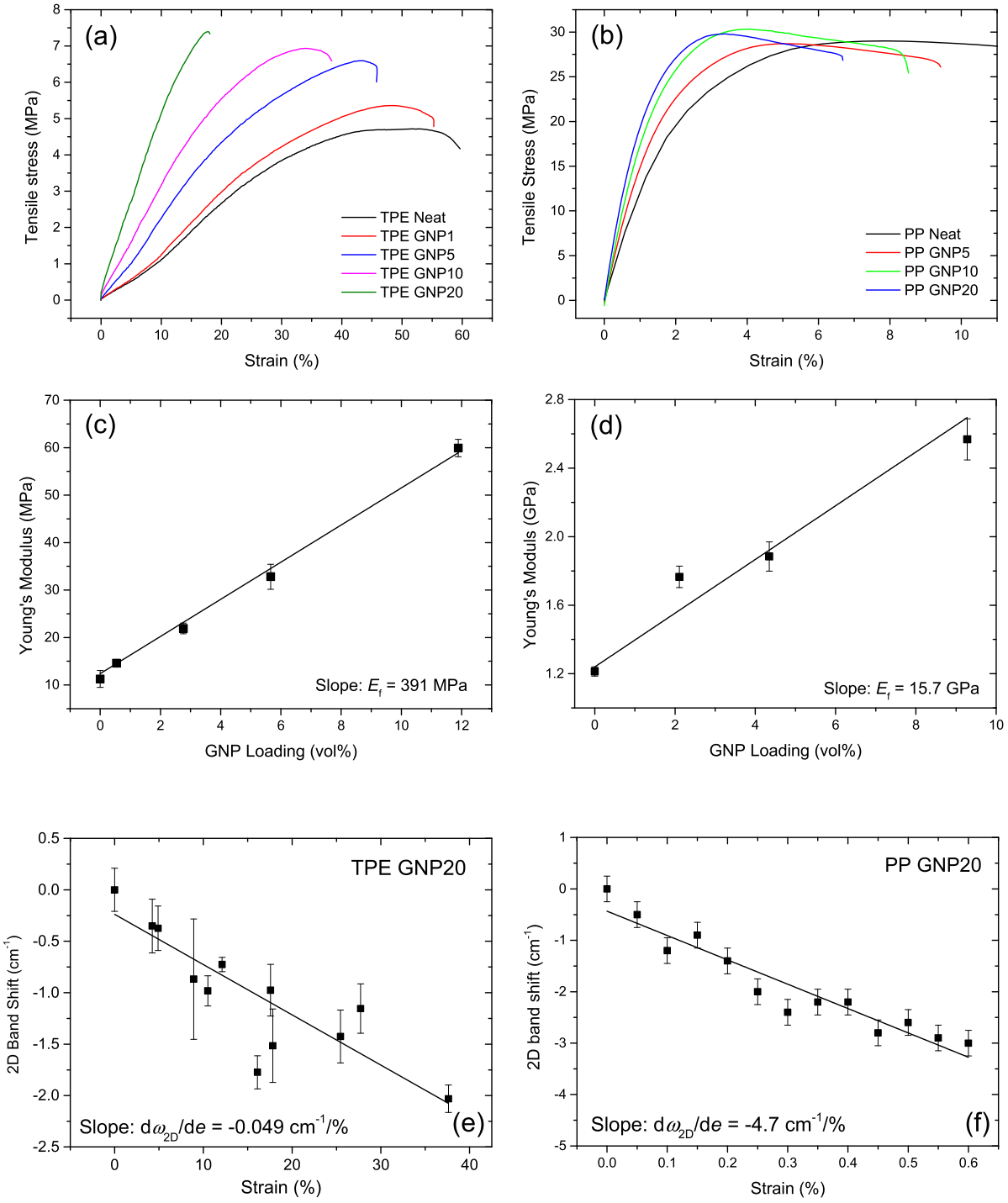

Fig. 1. Mechanical property data for nanocomposites consisting of M25 GNPs in TPE and PP matrices. (a) Stress-strain curves for the TPE with different loadings of GNPs in parts per 100 parts of rubber (phr). (b) Stress-strain curves for the PP with different loadings of GNPs in weight percent (wt%). (c) Dependence of the Young's modulus of the nanocomposite E_c upon V_f for the TPE. (d) Dependence of E_c upon V_f for the PP. (e) Dependence of the 2D Raman band position upon strain for 20 phr of the GNPs in the TPE. (f) Dependence of the 2D Raman band position upon strain for V_f ~10% of GNPs in the PP.

$$E_c = E_{eff}\eta_o\eta_l V_p + E_m(1 - V_p) \quad (2)$$

where η_o is the Krenchel orientation factor [15,16] and η_l is the length factor [17]. The parameter E_{eff} is the effective Young's modulus of the filler that depends only upon its structure. For example it will be 1050 GPa for monolayer graphene but will be lower for few-layer graphene [18,19] and graphene oxide [20,21]. The orientation factor η_o is 1 for aligned nanoplatelets and it was shown recently [15,16] that for randomly-oriented nanoplatelets, $\eta_o = 8/15$. The length factor η_l ($0 \leq \eta_l \leq 1$) reflects the efficiency of stress transfer from the matrix to the filler that is controlled by both the shape of the filler and the strength of the filler-matrix interface.

Stress transfer from the matrix to the individual aligned

Table 1
Summary of the matrix and filler modulus values determined for the different polymers from the mechanical testing and Raman band shifts.

Polymer matrix[a]	E_m (GPa)	E_f (GPa) (Mechanical)	$d\omega_{2D}/de$ (cm^{-1}/% strain)	E_R (GPa) (Raman)	Reference
Epoxy Resin 1	2.5	58 ± 10	4.0 ± 1.0	70 ± 17	Supplementary Data
Epoxy Resin 2	1.98	–	3.0 ± 1.1[a]	52 ± 20	Supplementary Data
Polypropylene	1.2	36 ± 5	4.0 ± 1.3	70 ± 22	This study
TPE 2 (Pebax)	0.45	13 ± 3	1.0 ± 0.5	17.5 ± 8.7	Supplementary Data
TPE 1 (Alcryn)	1.1×10^{-2}	0.52 ± 0.16	0.042 ± 0.017	0.73 ± 0.30	This study
Nitrile Rubber (NBR)	1×10^{-3}	0.035 ± 0.006	0.0074 ± 0.0028	0.13 ± 0.05	Supplementary Data
Natural Rubber (NR)	8.1×10^{-4}	0.054 ± 0.009	0.0068 ± 0.0017	0.12 ± 0.03	[10]

[a] (Determined from $2 \times d\omega_D/de$).

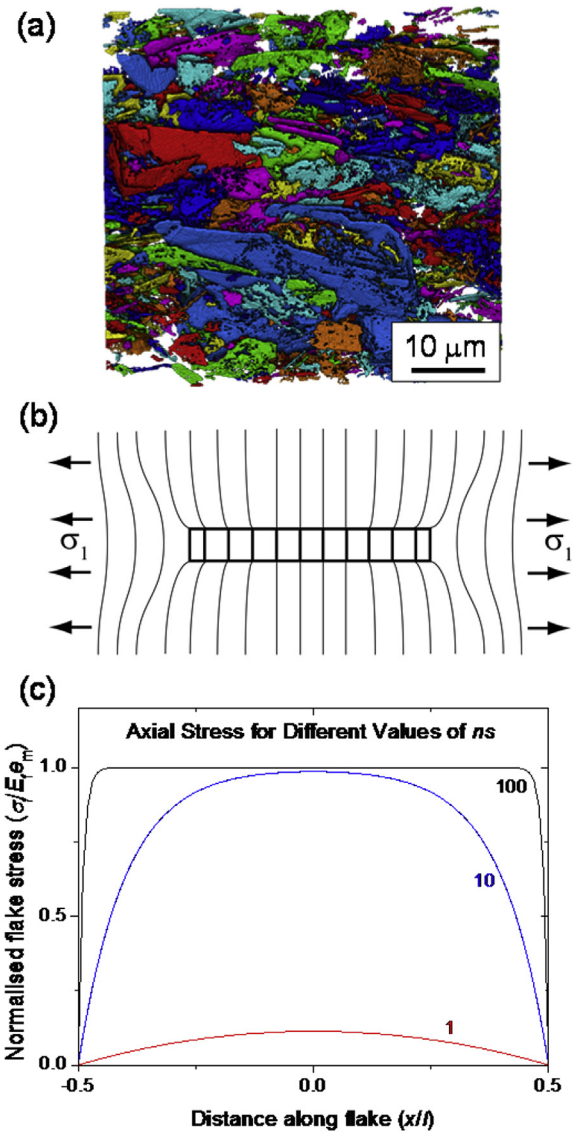

Fig. 2. (a) Artificially-coloured image of a CT scan of a natural rubber nanocomposite [13] containing M25 GNPs nanoplatelelets. (b) Deformation patterns for a discontinuous nanoplatelet in a polymer matrix under stress. (c) Predicted variation of normalized axial stress with distance along the nanoplatelet for a short nanoplatelet in a matrix. (The values of the product *ns* are indicated.)

nanoplatelet shown in Fig. 2(b) is assumed to take place through a shear stress at the nanoplatelet/matrix interface [6,9]. Before deformation, parallel lines perpendicular to the nanoplatelet can be drawn from the matrix through the nanoplatelet. When the system is subjected to axial stress, σ_1, parallel to the plane of the nanoplatelet, the lines become distorted as shown in Fig. 2(b) since the Young's modulus of the matrix is much less than that of the nanoplatelet. This induces a shear stress at the nanoplatelet/matrix interface. The axial stress in the nanoplatelet will build up from zero at the nanoplatelet ends to a maximum value in the middle of the nanoplatelet and shown in Fig. 2(c). The uniform strain assumption means that, if the nanoplatelet is long enough, the strain in the middle of the nanoplatelet equals that of the matrix. Since the nanoplatelets have a much higher Young's modulus than the matrix the nanoplatelets carry most of the load in the composite. It should be pointed out that this approach is different from that developed by Eshelby [22,23] and Tanaka and Mori [24] for a matrix reinforced by rigid inclusions. In our model there is a variation of stress along the nanoplatelets whereas the inclusion models assume a uniform stress within the nanoplatelets.

The behavior of a single discontinuous nanoplatelet in a matrix can be modelled using shear lag theory [8,9,17,25,26] in which it is assumed that the nanoplatelet of length l and thickness t is surrounded by a layer of resin with an overall thickness of T [9]. It is also assumed that both the nanoplatelet and matrix deform elastically and the nanoplatelet-matrix interface remains intact. The final equation for the distribution of nanoplatelet stress as a function of distance, x along the nanoplatelet at a given level of matrix strain, e_m, was determined in our earlier study and is given by Ref. [9].

$$\sigma_f(x) = E_{eff} e_m \left[1 - \frac{\cosh(nx/t)}{\cosh(nl/2t)}\right] \tag{3}$$

where $n = \sqrt{\frac{2G_m}{E_{eff}}\left(\frac{t}{T}\right)}$,

E_{eff} is the effective Young's modulus of the nanoplatelet and G_m is the shear modulus of the matrix. It is convenient to use the concept of nanoplatelet aspect ratio, $s = l/t$ so that the above equation can be rewritten as

$$\sigma_f(x) = E_{eff} e_m \left[1 - \frac{\cosh\left(ns\frac{x}{l}\right)}{\cosh(ns/2)}\right] \tag{4}$$

for the axial nanoplatelet stress. The effect of the different parameters upon the build-up of stress in a nanoplatelet is demonstrated in Fig. 2(c) for different values of the product *ns*. It can be seen that the nanoplatelet is most highly stressed, i.e. the most efficient reinforcement is obtained, when the product *ns* is high.

The mean stress along an aligned individual nanoplatelet can be determined from the integral

$$\overline{\sigma}_f = \frac{1}{l}\int_{-l/2}^{+l/2} \sigma_f(x)\, dx \tag{5}$$

Substitution of Equation (4) into this integral gives

$$\overline{\sigma}_f = E_{eff} e_m \left[1 - \frac{\tanh(ns/2)}{ns/2}\right] \tag{6}$$

This equation again shows that the best reinforcement is obtained when E_{eff} is high and the product ns is very large.

The Young's modulus of the nanoplatelet E_f in the nanocomposite is given by the mean stress $\overline{\sigma}_f$ divided by the nanoplatelet strain e_f (= e_m for uniform strain). Hence for an aligned individual nanoplatelet Equation (6) gives

$$E_f = E_{eff}\left[1 - \frac{\tanh(ns/2)}{ns/2}\right] \tag{7}$$

This shows that the value of E_f for an aligned graphene nanoplatelet in the nanocomposite is controlled by the effective Young's modulus of the nanoplatelet, E_{eff}, and the value of ns. It also follows that the length factor is given by

$$\eta_l = 1 - \frac{\tanh(ns/2)}{ns/2} \tag{8}$$

If the nanoplatelets are not aligned then the Krenchel orientation factor [15,16] needs to be taken into account and Equation (7) becomes

$$E_f = E_{eff}\eta_o\left[1 - \frac{\tanh(ns/2)}{ns/2}\right] \tag{9}$$

In the case where ns is small this equation can be recast since the hyperbolic function can be represented by a Taylor series as

$$\tanh x = x - \frac{x^3}{3} + \frac{2x^5}{15} - \frac{17x^7}{315} + \ldots\ldots\ldots\ldots \tag{10}$$

If ns is small Equation (9) then becomes

$$E_f \approx E_{eff}\eta_o\frac{(ns/2)^2}{3} \tag{11}$$

Substituting the value of n given in Equation (3), this gives for small values of n

$$E_f \approx \eta_o\frac{s^2}{6}\frac{t}{T}G_m \tag{12}$$

The shear modulus of the matrix is related to its Young's modulus through the relation [8].

$$G_m = \frac{E_m}{2(1+\nu)} \tag{13}$$

where ν is Poisson's ratio (typically ν ~ 0.35–0.5 for rigid polymers and elastomers). Combining Equations (12) and (13) gives the final equation

$$E_f \approx \eta_o\frac{s^2}{12}\frac{t}{T}\frac{E_m}{(1+\nu)} \tag{14}$$

Hence it is predicted that $E_f \propto E_m$ when ns is small corresponding, for a fixed aspect ratio s, to low values of G_m and hence E_m. Moreover the slope of unity on a log-log plot of E_f versus E_m is predicted, as found from the analysis of literature data [14] (see Fig. S1, Supplementary Information).

In a nanocomposite containing an array of nanoplatelets, the ratio t/T is related to the proximity of neighboring particles and hence the volume fraction of filler, V_f. The exact relationship will depend upon the geometry of the arrangement of the nanoplatelets and for the simple case of a stack of nanoplatelets sandwiched between layers of polymer matrix, it can be assumed that $t/T \sim V_f$. Using this relationship and substituting Equation (14) back into the rule of mixtures equation (1) gives

$$E_c \approx \eta_o\frac{s^2}{12}\frac{E_m}{(1+\nu)}V_f^2 + E_m\left(1 - V_f\right) \tag{15}$$

which on rearranging becomes

$$E_c \approx E_m\left[1 - V_f + \frac{s^2}{12}\frac{\eta_o}{(1+\nu)}V_f^2\right] \tag{16}$$

This equation, with the dependence of E_c upon both the square of the filler aspect ratio s^2 and V_f^2 and the independence of E_c upon E_f, is reminiscent of the Guth-Gold relationship often used to model the effect of the addition of fillers upon the stiffness of elastomers [27–29]. This gives further confidence in our use of the shear-lag approach.

Varying the parameters in Equation (9) reveals some interesting findings as discussed in detail in the Supplementary Information and shown in Fig. S2. The effect of varying the value of the effective filler modulus E_{eff} is shown in Fig. S2(a). A higher value of E_{eff} leads to a higher value of E_f for rigid matrix materials ($E_m > 1$ GPa) but for flexible matrices, E_f is independent of E_{eff} as predicted by Equation (14). The value of E_f depends upon the degree of orientation of the nanoplatelets as shown in Fig. S2(b); it is reduced by a factor of 8/15 for randomly oriented nanoplatelets compared with perfectly-aligned ones [15,16]. Fig. S2(c) shows that E_f depends strongly upon the aspect ratio, s, highlighting that the aspect ratio of the nanofiller is of vital importance. The dependence of E_c upon the diameter of the GNPs is shown in Fig. S4. Finally Fig. S2(d) shows that E_f depends strongly upon the ratio, t/T. This parameter essentially depends upon how rapidly the stress decays into the matrix away from the nanofiller and is controlled by both the volume fraction of filler and the strength of the filler-matrix interface. Hence this ratio, t/T, can be thought of as an indication of the quality of the interface [9] and E_f will be higher for stronger interfaces. The significance of all these different parameters upon the relationship between E_f and E_m is discussed in detail in the Supplementary Information.

It is also possible to use Equation (9) to model the reinforcement by the same graphene nanoplatelets of the different polymer matrices with different values of E_m presented in Table 1 and Fig. 1 as shown in Fig. 3. A plot of E_f versus E_m for the different systems investigated is given in Fig. 3(a) and the solid line is the fit of Equation (9) to the data using with appropriate values of the various parameters indicated in the Figure. A value of $E_{eff} = 350$ GPa was chosen to take into account the decrease in graphene modulus that occurs as the number of layers increases [18,19]. The same value of E_{eff} was used for the GNPs in the different matrix materials, implying that further exfoliation of the GNPs did not occur during processing. An aspect ratio of 2000 was used, along with a value of t/T of 2.5×10^{-4} although these parameters can be adjusted to modify the fit. In addition it was assumed that the nanoplatelets were randomly oriented so that $\eta_o = 8/15$ [15,16]. It can be seen that overall there is excellent agreement between the predicted and

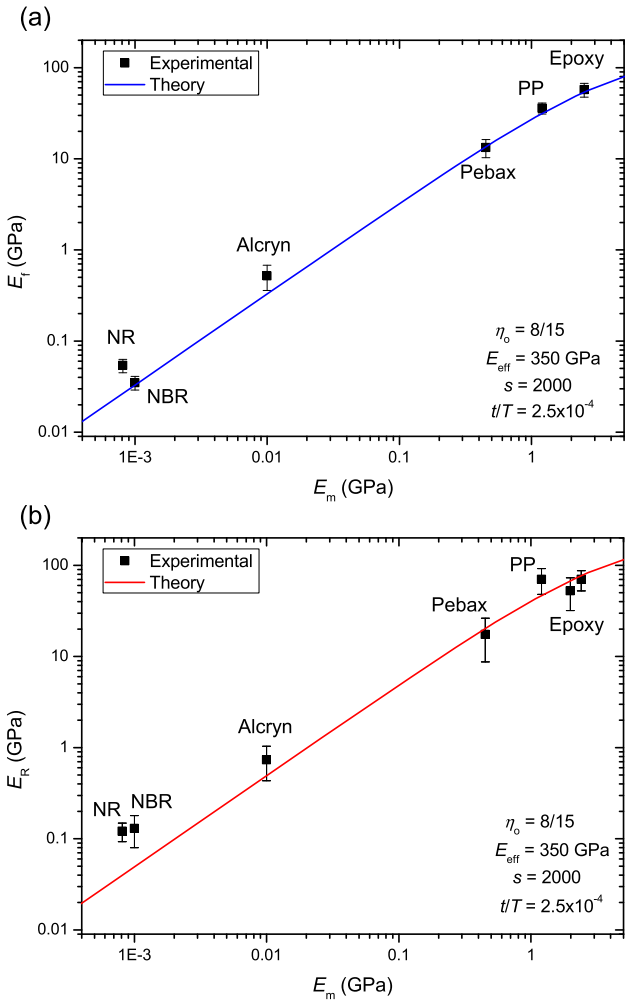

Fig. 3. (a) Variation of E_f with E_m for the M25 GNPs reinforcing a series of polymeric matrix different materials with different values of matrix modulus, E_m. The solid line is the behavior predicted using Equation (9) with the parameters indicated. (b) Variation of E_R with E_m for the GNPs reinforcing a series of polymeric matrix different materials with different values of matrix modulus, E_m. The solid line is the behavior predicted using Equation (16) with the parameters indicated.

measured values of E_f. The close correlation in Fig. 3(a) of E_f with E_m measured from bulk mechanical properties implies that molecular-scale interactions between the nanoparticles and polymer matrix [11,12], giving rise to phenomena such as tethering of molecular chains or local crystallisation, do not have a major effect upon the reinforcement mechanisms.

It should be pointed out that our analysis is only applicable to the prediction of E_f, the Young's modulus of the particulate filler, for use in Equation (1). Although this equation can then be used to predict the Young's modulus of the composite, E_c, the rule of mixtures often breaks down, typically through the agglomeration of the nanofiller particles, especially at high loadings. This is not the case in the two examples shown in Fig. 1, but agglomeration often occurs in thermosetting systems such as epoxy resins where a significant increase in E_c can be obtained for low loadings of graphene [30], and no further increase is found above a certain loading of the nanofiller (see Supplementary Information – Fig. S6).

Another interesting implication of the theory is that E_f increases as E_m increases. In the case of pure polymers E_m is generally no higher than around 5 GPa which limits the maximum value of E_f that can be obtained for polymer-matrix nanocomposites. This is not the case for metal matrix composites and a recent study [31] has shown that significant levels of reinforcement can be obtained for an aluminium matrix composite (E_m ~ 70 GPa) reinforced with graphene oxide.

3.3. Stress-induced Raman band shifts

It has been established by the authors that stress transfer from the matrix to the reinforcement in nanocomposites reinforced by graphene nanoplatelets (GNPs) can be followed from stress-induced Raman band shifts for the graphene [30,32,33]. The Young's modulus of graphene-based materials can be estimated from the slope of a plot of the 2D (or D) Raman band position against strain [34,35]. We shall term the modulus determined in this way in nanocomposites, the Raman modulus, E_R. It is well known that the 2D band for monolayer graphene with a Young's modulus of 1050 GPa subjected to tensile deformation downshifts by −60 cm^{-1}/% strain [34,35]. The rate of shift of the position of the 2D Raman band per unit strain ($d\omega_{2D}/de$) can then be used to determine the value of E_R for any type of graphene in a composite through the simple relation

$$E_R = \frac{d\omega_{2D}}{de} \times \frac{1050}{-60} \text{ GPa} \quad (17)$$

where $d\omega_{2D}/de$ is determined for the 2D band in cm^{-1}/% strain. A similar equation can be used for the shift rate of the D band, $d\omega_D/de$, with the −60 being replaced by −30.

The variation of the position of the 2D band with strain for GNPs in the TPE matrix is shown in Fig. 1(e) and the mean value of $d\omega_{2D}/de$ calculated from an average of at least 5 measurements for each system is given in Table 1. Similar measurements for the PP reinforced with GNPs are shown in Fig. 1(f) and the average value is also given in Table 1. In each case the value of E_R estimated using Equation (15) is also given in the Table and it can be seen that the values of E_f and E_R determined using the two independent techniques are similar for each material, with E_R generally being higher than E_f. It is shown in the Supplementary Information that it is possible modify the shear lag theory developed above to predict the dependence of E_R upon E_m as

$$E_R = \eta_o E_{eff}\left[1 - \frac{1}{\cosh(ns/2)}\right] \quad (18)$$

and the final equation for flexible polymers (E_m < 1 GPa) is

$$E_R \approx \eta_o \frac{s^2}{8}\frac{t}{T}\frac{E_m}{(1+\nu)} \quad (19)$$

Comparison of Equation (18) with Equation (9) shows that it is predicted that $E_R > E_f$, as is often found (Table 1).

It is also possible to use Equation (18) to model the Raman band shift rates of the different polymer matrices with different values of E_m presented in Table 1 and Fig. 1. Fig. 3(b) shows a plot of E_R versus E_m for the different systems investigated and the solid line is the fit of Equation (18) to the data using with appropriate values of the various parameters indicated in the Figure. It can be seen that there is again good agreement between the predicted and measured values of E_R.

4. Conclusions

In conclusion it is clear that the development of our simple but comprehensive theory has enabled the effective Young's modulus of graphene nanoplatelets in polymer-based nanocomposites to be

modelled with a high degree of precision. The importance of different structural parameters is clearly highlighted. The theory gives a convincing explanation of why it is not possible to realise the promised 1 TPa Young's modulus of the graphene in low modulus polymeric matrices. In fact it predicts, perhaps rather surprisingly, that the Young's modulus of such a nanocomposite will be independent of the Young's modulus of the nanofiller. In general it appears therefore that for most polymers, the aspect ratio of the nanoplatelets is more important than their Young's modulus. This is not a necessarily a drawback, however, in the case of graphene since this nanofiller generally has both a high Young's modulus and high aspect ratio. Two other parameters that are of vital significance are the orientation of the nanoplatelets and the strength of the interface with the matrix. Aligned nanoplatelets give a level of reinforcement roughly twice that of randomly-oriented ones. Also, not surprisingly, the theory shows that a strong nanofiller-matrix interface leads to good stress transfer and hence better reinforcment than a weak interface.

This theory does have it limtations, however. It is only concerned with the elastic deformation of the nanocomposites at relatively low levels of loading before any agglomeration or restacking effects occur. It is also not related directly to other important mechanical properties such as fracture strength, impact resistance or toughness. Nevertheless, the ability of nanofillers such as graphene to increase the stiffness of a polymer is of major technological importance and our theoretical approach represents a significant step forward towards a full understanding of the mechanical properties of polymer-based nanocomposties reinforced with nanoplatelets.

Acknowledgements

This research has been supported by funding from the European Union Horizon 2020 Programme under the Graphene Flagship grant agreement n°604391. One of the authors (M. Liu) is grateful to the China Scholarship Council for financial support. The authors are also grateful to Drs T. Burnett and T. Slater of the School of Materials for help with the CT scans. All research data supporting this publication are available within this publication.

Appendix A. Supplementary data

Supplementary data related to this article can be found at https://doi.org/10.1016/j.compscitech.2017.11.007.

References

[1] C. Lee, X. Wei, J.W. Kysar, J. Hone, Measurement of the elastic properties and intrinsic strength of monolayer graphene, Science 321 (5887) (2008) 385–388.
[2] U. Khan, P. May, A. O'Neill, J.N. Coleman, Development of stiff, strong, yet tough composites by the addition of solvent exfoliated graphene to polyurethane, Carbon 48 (14) (2010) 4035–4041.
[3] H. Kim, A.A. Abdala, C.W. Macosko, Graphene/polymer nanocomposites, Macromol 43 (16) (2010) 6515–6530.
[4] S. Biswas, H. Fukushima, L.T. Drzal, Mechanical and electrical property enhancement in exfoliated graphene nanoplatelet/liquid crystalline polymer nanocomposites, Compos Part A - Appl. Sci. 42 (4) (2011) 371–375.
[5] J.R. Potts, D.R. Dreyer, C.W. Bielawski, R.S. Ruoff, Graphene-based polymer nanocomposites, Polymer 52 (1) (2011) 5–25.
[6] R.J. Young, I.A. Kinloch, L. Gong, K.S. Novoselov, The mechanics of graphene nanocomposites: a review, Compos Sci. Technol. 72 (12) (2012) 1459–1476.
[7] D.G. Papageorgiou, I.A. Kinloch, R.J. Young, Graphene/elastomer nanocomposites, Carbon 95 (2015) 460–484.
[8] R.J. Young, P.A. Lovell, Introduction to Polymers, third ed., CRC Press, Boca Baton, Florida, USA, 2013.
[9] L. Gong, I.A. Kinloch, R.J. Young, I. Riaz, R. Jalil, K.S. Novoselov, Interfacial stress transfer in a graphene monolayer nanocomposite, Adv. Mat. 22 (24) (2010) 2694–2697.
[10] R.J. Young, L. Gong, I.A. Kinloch, I. Riaz, R. Jalil, K.S. Novoselov, Strain mapping in a graphene monolayer nanocomposite, ACS Nano 5 (4) (2011) 3079–3084.
[11] P. Calvert, Materials science - strength in disunity, Nature 357 (6377) (1992) 365–366.
[12] G. Marom, H.D. Wagner, Should polymer nanocomposites be regarded as molecular composites? J. Mater Sci. 52 (14) (2017) 8357–8361.
[13] S.H. Li, Z.L. Li, T.L. Burnett, T.J.A. Slater, T. Hashimoto, R.J. Young, Nanocomposites of graphene nanoplatelets in natural rubber: microstructure and mechanisms of reinforcement, J. Mater Sci. 52 (16) (2017) 9558–9572.
[14] D.G. Papageorgiou, I.A. Kinloch, R.J. Young, Mechanical properties of graphene and graphene-based nanocomposites, Prog. Mater Sci. 90 (2017) 75–127.
[15] Z.L. Li, R.J. Young, I.A. Kinloch, N.R. Wilson, A.J. Marsden, A.P.A. Raju, Quantitative determination of the spatial orientation of graphene by polarized Raman spectroscopy, Carbon 88 (2015) 215–224.
[16] Z.L. Li, R.J. Young, N.R. Wilson, I.A. Kinloch, C. Valles, Z. Li, Effect of the orientation of graphene-based nanoplatelets upon the Young's modulus of nanocomposites, Compos Sci. Technol. 123 (2016) 125–133.
[17] D. Hull, T.W. Clyne, An Introduction to Composite Materials, second ed., Cambridge University Press, Cambridge; New York, 1996.
[18] L. Gong, R.J. Young, I.A. Kinloch, I. Riaz, R. Jalil, K.S. Novoselov, Optimizing the reinforcement of polymer-based nanocomposites by graphene, ACS Nano 6 (3) (2012) 2086–2095.
[19] L. Gong, R.J. Young, I.A. Kinloch, S.J. Haigh, J.H. Warner, J.A. Hinks, et al., Reversible loss of bernal stacking during the deformation of few-layer graphene in nanocomposites, ACS Nano 7 (8) (2013) 7287–7294.
[20] C. Gomez-Navarro, M. Burghard, K. Kern, Elastic properties of chemically derived single graphene sheets, Nano Lett. 8 (7) (2008) 2045–2049.
[21] J.W. Suk, R.D. Piner, J.H. An, R.S. Ruoff, Mechanical properties of mono layer graphene oxide, ACS Nano 4 (11) (2010) 6557–6564.
[22] J.D. Eshelby, The determination of the elastic field of an ellipsoidal inclusion, and related problems, Proc. R. Soc. Lon Ser-A 241 (1226) (1957) 376–396.
[23] J.D. Eshelby, The elastic field outside an ellipsoidal inclusion, Proc. R. Soc. Lon Ser-A 252 (1271) (1959) 561–569.
[24] K. Tanaka, T. Mori, Hardening of crystals by non-deforming particles and fibres, Acta Metall. Mater 18 (8) (1970) 931–941.
[25] H.L. Cox, The elasticity and strength of paper and other fibrous materials, Brit J. Appl. Phys. 3 (1952) 72–79 (Mar).
[26] J.A. Nairn, On the use of shear-lag methods for analysis of stress transfer unidirectional composites, Mech. Mater 26 (2) (1997) 63–80.
[27] Y. Fukahori, A.A. Hon, V. Jha, J.J.C. Busfield, Modified Guth-Gold equation for carbon black-filled rubbers, Rubber Chem. Technol. 86 (2) (2013) 218–232.
[28] R.J. Young, P.A. Lovell, Introduction to Polymers, third ed., CRC Press, Boca Raton, 2011, p. 615.
[29] E. Guth, Theory of filler reinforcement, J. Appl. Phys. 16 (1) (1945) 20–25.
[30] C. Valles, F. Beckert, L. Burk, R. Mulhaupt, R.J. Young, I.A. Kinloch, Effect of the C/O ratio in graphene oxide materials on the reinforcement of epoxy-based nanocomposites, J. Polym. Sci. Pol. Phys. 54 (2) (2016) 281–291.
[31] P. Hidalgo-Manrique, S.J. Yan, F. Lin, Q.H. Hong, I.A. Kinloch, X. Chen, et al., Microstructure and mechanical behaviour of aluminium matrix composites reinforced with graphene oxide and carbon nanotubes, J. Mater Sci. 52 (23) (2017) 13466–13477.
[32] S.R. Ahmad, C.Z. Xue, R.J. Young, The mechanisms of reinforcement of polypropylene by graphene nanoplatelets, Mater Sci. Eng. B-Adv 216 (2017) 2–9.
[33] D.G. Papageorgiou, I.A. Kinloch, R.J. Young, Hybrid multifunctional graphene/glass-fibre polypropylene composites, Compos Sci. Technol. 137 (2016) 44–51.
[34] C.A. Cooper, R.J. Young, M. Halsall, Investigation into the deformation of carbon nanotubes and their composites through the use of Raman spectroscopy, Compos Part A - Appl. Sci. 32 (3–4) (2001) 401–411.
[35] O. Frank, G. Tsoukleri, I. Riaz, K. Papagelis, J. Parthenios, A.C. Ferrari, et al., Development of a universal stress sensor for graphene and carbon fibres, Nat. Commun. 2 (2011) 255.